Longitudinal acoustic mode in polymers: Influence of defects

Chih Chang and S. Krimm

Department of Physics, Macromolecular Research Center and Biophysics Research Division, University of Michigan, Ann Arbor, Michigan 48109

Normal mode calculations have been done on planar zigzag chains C_n ($n = 22$ to 82), terminated or connected by various fold structures and subjected to force and mass perturbations, to determine how the longitudinal acoustic mode (LAM) is influenced by such defects. We find that in general LAM-like displacements are distributed over a frequency range (depending on the stem length), with a total intensity smaller than that for the unperturbed case. Only when the fold comprises ~3% or less of the mass of the stem does it behave like a point mass perturbation. These results show that the perturbed elastic rod model has limited validity and that caution is necessary in attributing the shape of a LAM band entirely to a distribution of stem lengths.

PACS numbers: 43.20.Ks, 61.40.Km

INTRODUCTION

Since the first proposal[1] that a Raman-active longitudinal acoustic mode (LAM) occurs in the spectra of planar zigzag chains, two approaches have developed to understand how this phenomenon is related to the properties of the molecules. In the first, the molecular chain is considered to be an elastic rod,[1] whose unperturbed frequency $v_m = (m/2L)(E/\rho)^{1/2}$ is given in terms of the mode order m (an odd integer), the rod length L, the elastic modulus E, and the density ρ. This approach has been widely used: in the above application to a homogeneous unperturbed rod,[1,2] to a composite amorphous-crystalline rod,[3] in the approximation of a homogeneous rod with small force perturbations at the ends,[4] to composite rods with unrestricted mass and force perturbations at the ends,[5-9] and as the basis for treating coupled rods without[10] and with[11] damping in the connecting amorphous regions. The elastic rod model has also been used for analyzing LAM intensities in unperturbed rods,[12,13] thereby providing a basis for determining straight chain segment length distributions in polyethylene.[12]

At the same time it has been recognized that the LAM corresponds to a normal mode of the molecule, and should therefore be better understood from the results of calculations of such vibrations. In this second approach, whether based on a linear[2] or planar zigzag[14] point mass model, frequencies, and eigenvectors can be obtained for the LAM-like modes, and from the eigenvectors the intensities can be calculated.[15,16] Taken together, these properties should provide greater insight into the factors determining the observed LAM bands.

The goal of using the LAM to study the morphology of polyethylene has been the hope that the technique would provide direct information on the all-*trans* segment lengths in the specimen. It is clear that, since polymers are molecules that from a crystallographic point of view inherently have defects, this goal will not be realized until we have a detailed understanding of how such (conformational) defects influence the LAM. This must ultimately be obtained from normal mode analyses; indeed we will show that predictions of the elastic rod model can be incorrect. Normal mode analyses have been given for some internal conformational[15] and branch[17] defects. We have initiated a more extensive study

involving a broader range of defect structures.

We begin by considering the generalized predictions of the elastic rod with force and mass perturbations. We then examine the results of normal mode calculations on structures that implicitly and explicitly model these as well as structural defects. The basic result that emerges is that the LAM of the straight chain segment depends on how effectively its vibrations are coupled to those of the defect. As we will see, this varies with the length of the straight chain and the nature of the defect.

PREDICTIONS OF ELASTIC ROD MODEL

It will be useful to examine whether the elastic rod model provides a satisfactory description of frequencies and intensities even in the limit of small perturbations. We assume a rod of length L, cross-sectional area A, elastic modulus E, and density ρ, with point masses M at each end and force perturbations at the ends represented by force constants f. Any mode can be characterized by a wavevector k_m and frequency ω_m related by

$$\omega_m = v k_m, \tag{1}$$

where v, the wave velocity along the axial direction, is given by

$$v = (E/\rho)^{1/2}. \tag{2}$$

For an unperturbed rod, $k^0_m = m\pi/L$, $m = 1,3,5....$

The longitudinal displacement in a normal mode satisfies a wave equation that leads to the condition[6]

$$\cot\left(\frac{k_m L}{2}\right) = \frac{M\omega^2 - f}{AEk_m}. \tag{3}$$

If the perturbations are small, we can expand around the unperturbed value, i.e., $\cot(k_m L/2) = 0$. This gives

$$\frac{d}{dk_m}\cot\left(\frac{k_m L}{2}\right)\Delta k_m = \frac{M\omega^2 - f}{AEk_m}, \tag{4}$$

from which

$$\frac{k_m L}{2} = \frac{m\pi}{2} + \frac{f - M\omega^2}{AEk_m}. \tag{5}$$

Solving for k_m, and expanding the square root, with neglect of higher order terms in f and M, gives

$$k_m = \frac{m\pi}{L + \dfrac{2M}{A\rho}} + \frac{2f}{m\pi AE}$$

$$= k_m^0\left(1 - \frac{2M}{M_T} + \frac{2fL}{(m\pi)^2 AE}\right), \tag{6}$$

where in the second form higher order terms in $2M/M_T$ (M_T is the total mass of the rod) have been neglected. The frequency $\nu_m = \omega_m/2\pi$ is

$$\nu_m = \nu_m^0\left(1 - \frac{2M}{M_T} + \frac{2fL}{(m\pi)^2 AE}\right), \tag{7}$$

where

$$\nu_m^0 = (m/2L)(E/\rho)^{1/2}. \tag{8}$$

There is abundant evidence for the frequency increase due to small perturbing forces acting at the ends of n-paraffin chains.[4,7,9] The frequency decrease due to the mass effect has also been shown to occur in a cyclic paraffin and in perfluoro n-alkanes.[18] It is worth noting that if both effects are present simultaneously they could cancel each other and give the appearance of an absence of perturbations in the $m = 1$ mode (but not in higher order modes).

The LAM intensity can be obtained by a treatment similar to that previously given for an unperturbed rod.[13] The polarizability change α' is related to the displacement in the rod, $u(x) = B\sin(k_m x)$, through the internal strain:

$$\alpha' = \int_{-L/2}^{L/2} \alpha_0 \frac{\partial u}{\partial x} dx$$

$$= \int_{-L/2}^{L/2} \alpha_0 B k_m \cos(k_m x) dx$$

$$= \frac{2\alpha_0 e_0}{k_m}\sin\left(\frac{k_m L}{2}\right), \tag{9}$$

where $e_0 = B k_m$ is the strain amplitude at $x = 0$ and α_0 is a constant related to the unit polarizability of the rod. The intensity is proportional to $(\alpha')^2$, and the mean square strain amplitude $\langle e_0^2 \rangle$ is obtained from the equipartition theorem. Thus:

$$\langle U \rangle = \frac{1}{2}k_B T$$

$$= \frac{1}{2}f_0 \int_{-L/2}^{L/2} [e_0 \cos(k_m x)]^2 dx$$

$$= \frac{f_0 \langle e_0^2 \rangle}{4k_m}[k_m L + \sin(k_m L)], \tag{10}$$

where f_0 is an internal force constant. Substituting e_0 into the expression for $(\alpha')^2$ gives

$$(\alpha')^2 = \frac{8\alpha_0^2 k_B T}{f_0}\frac{\sin^2(k_m L/2)}{k_m[k_m L + \sin(k_m L)]}, \tag{11}$$

which in the absence of perturbations (i.e., $k_m = k_m^0 = m\pi/L$) reduces to

$$(\alpha')_0^2 = \frac{8\alpha_0^2 k_B T}{f_0}\frac{L}{(m\pi)^2} \tag{12}$$

as obtained earlier.[13] If the perturbation is small, we can expand $(\alpha')^2$ around $(\alpha')_0^2$:

$$(\alpha')^2 = (\alpha')_0^2 + \left(\frac{\partial(\alpha')^2}{\partial k_m}\right)_{k_m = k_m^0}(k_m - k_m^0), \tag{13}$$

and we find that

$$(\alpha')^2 = (\alpha')_0^2\left(1 + \frac{2M}{M_T} - \frac{2fL}{(m\pi)^2 AE}\right). \tag{14}$$

Thus, the perturbations influence the intensities in a manner opposite to that of the frequencies.

Is Eq. (14) consistent with observation? As has been noted,[13] the scattered intensity from a n-paraffin sample is proportional not only to the scattering per molecule but also to the molecular density in the sample ρ_s. Thus, for LAM-1 (i.e., $m = 1$)

$$I(\text{LAM}) \propto (\alpha')^2 \cdot \rho_s \propto L\left(1 + \frac{2M}{M_T} - \frac{2fL}{\pi^2 AE}\right)\cdot\rho_{CH_2}\frac{L_{CH_2}}{L}, \tag{15}$$

where ρ_{CH_2} is the density of the CH_2 groups in the sample and L_{CH_2} is the length per CH_2 group along the chain. Since ρ_{CH_2} is essentially constant for all crystalline n-alkanes, it was expected that the LAM intensities would be independent of chain length [as can be seen from Eq. (15) for an unperturbed chain]. Measurements on n-paraffins from $C_{30}H_{62}$ to $C_{80}H_{162}$ showed the intensities to be constant to within about 3%. In fact, we already know that n-paraffins exhibit end force perturbations in their frequencies,[4,7,9] and we should therefore expect Eq. (15) to apply. This predicts an intensity decrease of about 8% over the above range of chain lengths for typical values of f^7.

It would thus seem that as far as intensities are concerned the elastic rod may be a poor model for real molecules. In fact, we will also see that, whereas the intensity decrease for force perturbations is qualitatively correct in terms of the results of normal mode calculations, the intensity increase predicted for mass perturbations is incorrect. The essential problem is that in the elastic rod, despite the perturbations, the longitudinal displacements are confined to a single mode at one frequency (for a given m). In a real molecule, on the other hand, the LAM-type motion can be distributed among a number of normal modes, being mixed (depending on the perturbations) with other coordinates. It is therefore important to understand in greater detail how specific kinds of departures from unperturbed straight chains influence the LAM frequency and intensity. An approach has recently been developed in terms of generalized properties of the straight chains and attached structures.[19] Our approach has been to examine the behavior of specific structures through complete normal mode calculations.

CALCULATIONS

Defect structures

A variety of nonplanar zigzag structures, most chosen from the literature,[20-24] formed the basis for the model structures of defective planar zigzag systems that we calculated. These nonregular defect conformations are listed in Table I; the specific model structures will be given below.

Force perturbations were studied for some of the systems, and these were modeled by introducing an additional

TABLE I. Nonregular conformations used to model defective planar zigzag polymethylene systems.

Symbol	Type	Conformation[a]	Reference
F_1	(110)fold	200°, 248°, 77°, 86°, 206°, 82°, 235°	22
F_A	(110)fold	$gt_3 g_2 t g_2 t_2 g$	21
F_B	(110)fold	$(gtg't)_2 gtg_2 tg_3 (tg'tg)_2$	21
F_C[b]	(110)fold	112.8°, 112.1°, 113.6°, 112.7°, 114.8°, 114.8°, 116.2°, 114.0°, 111.4°, 113.5°; 184.5°, 176.7°, 74.9°, 174.8°, 68.4°, 91.6°, − 58.4°, − 64.4°, 174.4°, 171.3°, 180.4°	20
F_4	(110)fold	$ggtggt$	23
F_0	(110)fold	$gtg'(tg)_2 gtggg$	24
D	defect	$gtgg_2^+ t$	
J	(110)jog	166°, 43°, 173°, 173°, 132°, 69°, 197°	22
K	kink	279°, 245°, 285°, 148°, 201°, 189°, 130°	22

[a] Given in terms of dihedral angles (in degrees, or *trans* and gauche), except for F_C, where the first group represents bond angles.

[b] F_C is the structure used for fold. Torsions of this conformation have been used as terminal structure, as follows: F_C^*—114.8, 114.8, 116.2, 114.0, 111.4, 113.5; 68.4, 91.6, − 58.4, − 64.4, 174.4, 171.3. F_C^+—112.8, 112.1, 113.6, 112.7, 114.8, 114.8; 176.7, 74.9, 174.8, 68.4, 91.6, − 58.4.

pseudobond, attached to a mass of 10^4 amu, at the atom where the force is acting. Since the large mass hardly moves during the vibration, the molecule now vibrates mainly under the influence of the interaction force constant experienced by the atom to which the pseudobond is attached. Mass perturbations were modeled by increasing the masses of particular atoms.

Frequencies

The normal modes of the complete structure were calculated in the approximation of the CH_2 group being taken as a point mass of 14.001 amu (a terminal CH_3 group being 15.001 amu). This is not expected to alter the validity of the calculations: we are interested only in skeletal modes, for which the force field was developed in a point mass approximation,[14] and we are more interested in the general trends rather than exact numerical results.

In addition to the force constants developed for a point mass planar zigzag polymethylene chain,[14] we added a force constant for the CCC–CCC' gauche interaction, since such conformations occur in our defect structures. This constant was obtained by fitting the frequencies of skeletal modes calculated for $(tg)_\infty$,$(tgtg')_\infty$, and $(g)_\infty$ structures in polyethylene,[25] and was determined to be − 0.05 mdyn Å/rad. In fact, the frequencies of the LAM-like modes are not sensitive to this force constant, but are influenced more by the torsional force constant. We fitted this force constant to the above structures, and obtained a value of 0.045 mdyn Å/ rad; this value was used for *trans* and gauche bonds.

Intensities

Intensities of the LAM-like modes can be calculated by a dot product or bond polarizability method.[16] In the former a dot product is taken between the displacement vector formed from the normalized atomic displacements in the

TABLE II. Calculated properties of C_n planar zigzag chains.[a]

n	$\nu(LAM)_0$	$\nu(rod)_0$	$(\bar{a}')_0^2$	$n(\bar{a}')_0^2$	β_3
22	102.9	106.4	0.0743	1.635	2.94
24	94.4	97.2	0.0669	1.606	2.93
36	63.2	63.8	0.0454	1.634	2.97
46	49.6	49.7	0.0359	1.651	2.98
58	39.4	39.2	0.0282	1.636	2.99
74	30.9	30.6	0.0223	1.650	2.99
82	28.0	27.6	0.0201	1.648	2.98

[a] $\nu(LAM)_0$ is the LAM-1 frequency, in cm^{-1}, obtained from the normal coordinate calculation.

$\nu(rod)_0$ is the LAM-1 frequency in cm^{-1}, obtained from Eq. (6), using $E = 2.90 \times 10^{12}$ dyn/cm^2 from Ref. 4.

$(\bar{a}')_0^2$ is the squared molecular polarizability derivative, calculated by the bond polarizability method (Ref. 16).

$\beta_3 = \nu(LAM\text{-}3)/\nu(LAM\text{-}1)$.

chain axis direction of the unperturbed LAM and the similar vector for the mode in question; this method therefore yields relative intensities. The bond polarizability method yields absolute intensities. We have used both methods to calculate the intensities of LAM-like modes. The dot product method generally yields lower values than the bond polarizability method, and does not have as strong a theoretical basis. We therefore give here only the results of the bond polarizability method.

PLANAR ZIGZAG CHAINS WITH FREE ENDS

In order to study the influence of defect structures on the LAM, it is necessary to know the characteristics of the unperturbed molecules. In our studies we varied the length of the planar zigzag segment from 22 (C_{22}) to 82 (C_{82}) methylene units, and in Table II we present some of the calculated properties of such all-*trans* chains. In Fig. 1 we show the atomic displacements for C_{22} in LAM-1 (102.9 cm^{-1}) and in two nearby transverse acoustic modes (TAM), which will be relevant to the subsequent discussion.

As can be seen from Table II, there is excellent agreement between $\nu(LAM)_0$ and $\nu(rod)_0$ for chains longer than
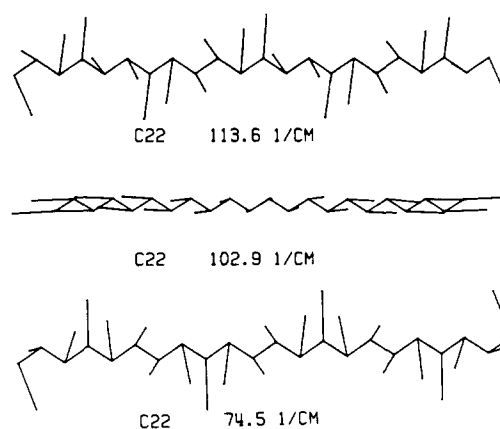

C22   113.6 1/CM

C22   102.9 1/CM

C22   74.5 1/CM

FIG. 1 Atomic displacements in LAM (102.9 cm^{-1}) and two nearby TAM modes of C_{22}.

TABLE III. Calculated properties of F_C^*-C_n-$F_C^\dagger$ chains.[a]

n	ν(LAM)	β_1	β (rod)	$(\bar{a}')_L^2$	I_L	I_T	$nI_T(\bar{a}')_0^2$	$\Delta\nu$
22	82.3	0.80	0.67	0.0171	23	68	1.11	68
24	74.6	0.79	0.68	0.0168	25	70	1.12	63
36	55.7	0.88	0.75	0.0121	27	75	1.23	37
46	46.7	0.94	0.80	0.0104	29	80	1.32	29
58	36.2	0.92	0.84	0.0130	46	81	1.32	20
74	29.0	0.94	0.86	0.0143	64	85	1.41	11
82	25.9	0.93	0.88	0.0105	52	86	1.42	7

[a] ν(LAM) is the LAM-1 frequency, in cm^{-1}, of the most LAM-like mode.

$\beta_1 = \nu$(LAM)/ν(LAM)$_0$ (cf. Table II).

β (rod) = ν(rod)/ν(rod)$_0$, where ν(rod) is calculated on the basis that F_C is a point mass (see Ref. 6).

$(\bar{a}')_L^2$ is the squared polarizability derivative of the most LAM-like mode.

$I_L = (\bar{a}')_L^2/(\bar{a}')_0^2$, in %.

$I_T = (\bar{a}')_T^2/(\bar{a}')_0^2$, where $(\bar{a}')_T^2$ represents the summed squared polarizability derivatives for all the LAM-like modes with intensities $\geqslant$1% of ν(LAM)$_0$.

$\Delta\nu$ is the frequency range for all the LAM-like modes with intensities $\geqslant$1% of ν(LAM)$_0$.

C_{36}, provided we use the value of E after correction for force perturbations in crystalline n-alkanes.[4] In this range of chain length the frequency ratio of LAM-3 to LAM-1 is close to 3, a characteristic of the unperturbed elastic rod. The square of the mean molecular polarizability derivative should be proportional to $1/n$, as has been shown for simple linear chains,[2] and this is seen to be true except for C_{24}, where the LAM-1 is mixed slightly with TAM-5.

It should be noted that the intensity scattered by a molecule is given, quantum mechanically, by[26]

$$I \propto \frac{(\nu_0 - \nu)^4 \, (\bar{a}')^2}{\nu[1 - \exp(-h\nu/k_B T)]}, \quad (16)$$

where $\nu_0 > \nu$ is the frequency of the incident radiation. For small ν the bracketed term is proportional to ν, and if we assume the relation between ν and L for an unperturbed rod, Eq. (6), we find that Eq. (14) reduces to $I \propto L$, the classical result of Eq. (10).

PLANAR ZIGZAG CHAINS WITH TERMINAL STRUCTURES

LAM as a function of chain length

We have examined two aspects of how the LAM of a planar zigzag segment is affected by nonregular terminal structures: the variation with chain length for a constant terminal structure, and the variation with terminal structure for a constant chain length. We first examine the former case.

The systems chosen for study were F_C^*-C_n-$F_C^\dagger$ chains in which n varies from 22 to 82 and F_C^* and $F_C^\dagger$ are parts of a (110) fold structure (cf. Table I); some of the results are given in Table III. The loss of planar symmetry and the coupling to the terminal structures causes the LAM of the all-*trans* segment to no longer be as well defined as in the unperturbed system. More than one mode in the vicinity of ν(LAM)$_0$ has LAM-like longitudinal displacements. We illustrate in Fig. 2 the three most intense such modes for F_C^*-C_{22}-$F_C^\dagger$, and the resemblance of these vibrational patterns to those of C_{22}

(Fig. 1) is obvious. The vibrational patterns of longer chains show similar features; they can be found in Ref. 27. In Fig. 3 we show the calculated LAM spectra for the above molecules for frequencies whose relative intensity is $\geqslant$1% of ν(LAM)$_0$. In Table III we list the frequency and intensity of the most LAM-like mode, the total intensity of LAM-like modes with relative intensity of $0.01I$ [ν(LAM)$_0$] or greater, and the frequency range over which these modes occur.

A number of interesting observations emerge from the above results. First, as expected, ν(LAM) is lower than ν(LAM)$_0$, although not by as much as is predicted from the
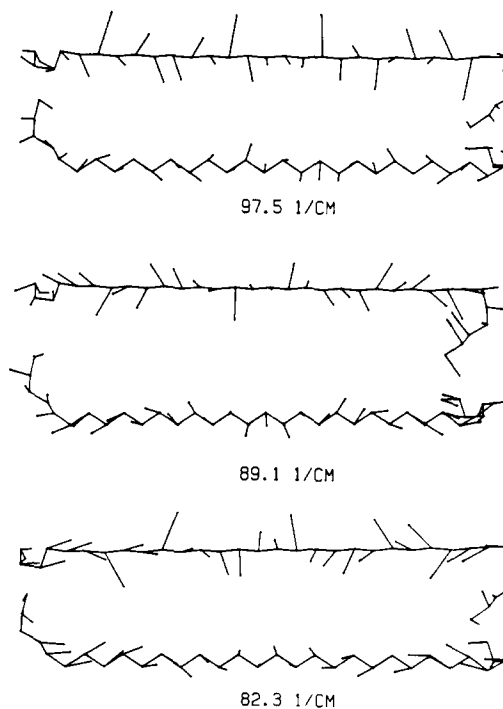

97.5 1/CM

89.1 1/CM

82.3 1/CM

FIG. 2. Atomic displacements in three most intense LAM-like modes of F_C^*-C_{22}-$F_C^\dagger$.

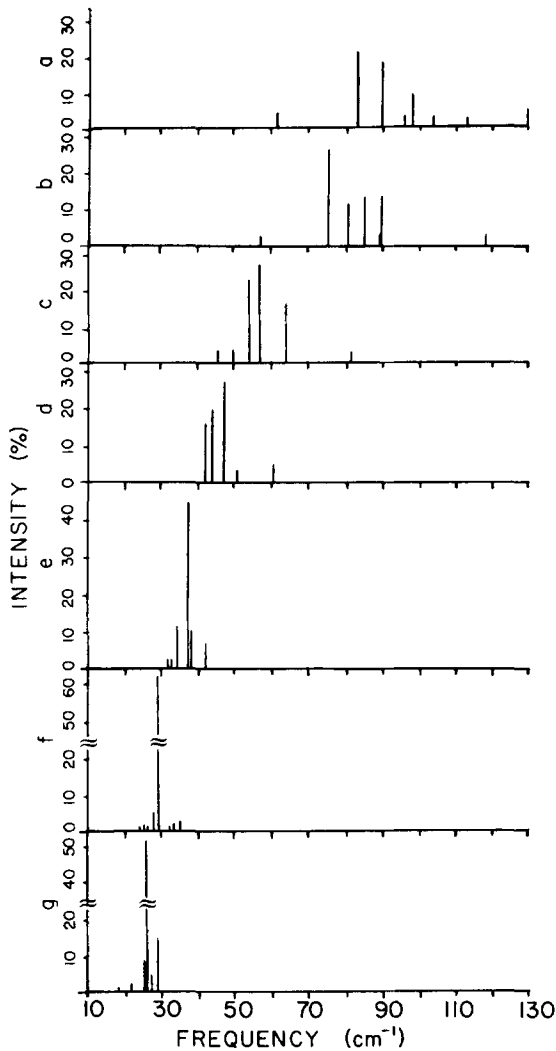FIG. 4. Frequency range (Δv) and total intensity (I_T) as a function of n for $F^*_C-C_n-F^\dagger_C$.

FIG. 3. LAM spectra for $F^*_C-C_n-F^\dagger_C$. (a) $n = 22$; (b) $n = 24$; (c) $n = 36$; (d) $n = 46$; (e) $n = 58$; (f) $n = 74$; (g) $n = 82$.

elastic rod model with the F^*_C or $F^\dagger_C$ structure taken as a point mass equivalent to 6 CH_2 groups [cf. the β_1 and β (rod) values in Table III]. This difference gets relatively smaller as n increases, indicating that the terminal structure behaves increasingly as a point mass. Second, not only is the intensity of $v(LAM)$, I_L, significantly lower than that of $v(LAM)_0$ (with fluctuations that depend on details of coupling with nearby modes), but I_L is no longer inversely proportional to n. In fact, even I_T (the sum of intensities of all LAM-like modes with $I_L \geqslant 0.01I$ $[v(LAM)_0]$), while increasing with n does not show this proportionality until higher values of n. Third, although the number of LAM-like modes is relatively constant with n (at about 6), these modes are found over a frequency range Δv that is large and decreases rapidly with increasing n.

The last two points raise the possibility of defining a value of n above which, for this terminal structure, the chain would behave as a simple mass-perturbed elastic rod. In Fig. 4 we show Δv and I_T as a function of n. By extrapolation, $\Delta v = 0$ near $n = 100$ and $I_T = 100\%$ near $n = 160$. Of course, both curves should give the same value of, and if we had included modes with $I_L < 0.01I$ $[v(LAM)_0]$ it is clear
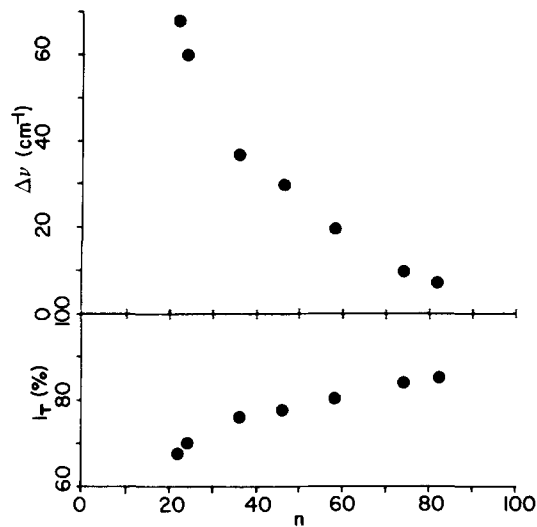
that both curves would shift in a direction to do so. For $n = 160$, the F^*_C (or $F^\dagger_C$) structure represents 3.8% of the mass of the trans stem; an elastic rod analysis[6] gives $\beta_1 = 0.93$, the asymptotic value that we find for $v(LAM)$ at n values very far from where the terminal structure behaves like a point mass.

The effect of the terminal structure on the LAM of the trans segment depends on how the vibrations of the former couple with those of the latter. An examination of the vibrational patterns of the modes represented in Fig. 3 shows that the units of F^*_C or $F^\dagger_C$ near the joint tend to vibrate longitudinally with the trans segment unless a sharp turn, i.e., a gauche bond, intervenes. Even so, the gauche bond does not decouple the rest of F^*_C and $F^\dagger_C$ from the trans segment, it just interrupts the continuity of the LAM motion. In the lower frequency LAM-like modes, units of F^*_C or $F^\dagger_C$ near the joint move in the same direction as end units of the trans segment; in the higher frequency LAM-like modes the corresponding displacements are in opposite directions. The relative vibrational amplitudes in the F^*_C or $F^\dagger_C$ and C_n components are not significantly different; thus, the noncrystalline region does not seem to contain as disproportionate a fraction of the vibrational energy as may be indicated by the composite rod model.[10,11] It should be noted that the connection between F^*_C (or $F^\dagger_C$) and the trans segment leads to a modification in the modes of the isolated F^*_C (or $F^\dagger_C$) structure. Therefore, the recent suggestion[19] that a terminal structure can be considered as a point mass as long as its lowest normal mode frequency is higher than $v(LAM)_0$ of the trans segment cannot be exactly correct. For example, this would be the case for structures longer than $F^*_C-C_{58}-F^\dagger_C$, but as we have seen, Δv and I_T considerations show that we are still far from being able to take the terminal structure as a point mass (although, interestingly, β_1 has reached the value that it has for $n = 160$ with the end structures taken as point masses). The discrepancy may be due to the neglect of transverse displacements in the rod.[19]

TABLE IV. Calculated properties of A–C_{74}–B chains.[a]

A	B	ν(LAM)	β_1	I_L	I_T	$\Delta\nu$	β_3
F'_0	F_0	27.5	0.89	55	75	10	3.27
$F'_0/2$	$F_0/2$	27.9	0.90	73	79	5	3.23
$t_s g$	$g t_s$	28.4	0.92	59	88	13	3.23
F^*_C	$F^\dagger_C$	29.0	0.94	64	85	11	2.86
F'_4	F_4	31.2	1.01	37	84	21	2.97
D'	D	31.4	1.02	50	88	18	2.92

[a] $A = F^*_C$ and $B = F^\dagger_C$ are taken from Table III. The prime indicates a reverse order to the dihedral angles $F_0/2$ represents half of the F_0 structure, viz., $gtg'tgt$. Other symbols are defined in Table III.

We therefore find that terminal nonregular structures cause the *trans* segment to vibrate in a few LAM-like modes with reduced intensities. These modes cover a large frequency range and are expected to give rise to an asymmetric band envelope. The range decreases, and the intensities increase, with increasing *trans* length, and when the terminal structure contains less than about 4% of the mass of the trans segment the specific vibrational coupling becomes negligible and the former structure can be taken as a point mass.

LAM as a function of terminal structure

We now examine how the LAM of the *trans* segment is influenced by the details of the terminal structure. For this purpose we have calculated the modes of A–C_{74}–B, where A and B are different end structures of 6 CH_2 groups (except F_0, which has 12). We present the characteristics of these molecules in Table IV and give their LAM spectra in Fig. 5.

Although all of the terminal structures (except F_0) contain 6 CH_2 groups, ν(LAM) is quite different. We have arbitrarily ordered the entries in Table IV in sequence of increasing ν(LAM), but in fact there seems to be a reason for this: while in all cases the terminal bond of the *trans* segment is gauche, the "extension" of the terminal structures generally decreases from F_0 to D. It seems as if the LAM mode can be carried more easily into an extended terminal structure than into a collapsed one. However, this is not the only determining feature, and the specific structure certainly plays a role. In fact, ν(LAM) for F_4 and D are even higher than ν(LAM-1) for C_{74}. (Note that the relationships of Table IV hold even if intensity-weighted LAM bands from Fig. 5 are used.) We also see that ν(LAM-3) is affected differently than ν(LAM-1), as is expected for perturbed systems, whether for small [cf. Eq. (7)] or large[8] perturbations. The intensities of the most LAM-like mode I_L seem to vary widely and in no regular fashion, although the total intensity I_T tends to increase as "extension" decreases. Note that this is the opposite of what is predicted for the elastic rod with small perturbations [Eqs. (7) and (14)].

The fact that the results for $F_0/2$ are very similar to those for F_0 led us to inquire whether further truncation of the terminal structure had any effect. Calculations in which the above structures were truncated to 3 CH_2 groups gave LAM spectra with many similarities to those in Fig. 5, with ν(LAM) being slightly closer to ν(LAM)$_0$. It seems as if ν(LAM) is most sensitive to the structure of the first few

groups beyond the *trans* stem, and hardly at all sensitive to the structure beyond about 6 groups.

Finally, since the length dependence of $\Delta\nu$ and I_T given in Fig. 4 pertained only to F^*_C and $F^\dagger_C$ terminal structures, it is clear that our estimate of the decoupled limit needs reconsideration. If we assume that relations of the form given in Fig. 4 are still valid for the other terminal structures, then the data of Table IV lead to the rough conclusion that $\Delta\nu = 0$ and $I_T = 100\%$ at about $n = 190$. This implies that the chain behaves like a mass-perturbed elastic rod only for terminal structures whose mass is about 3% or less of that of the *trans* segment. For shorter chains we expect the frequen-
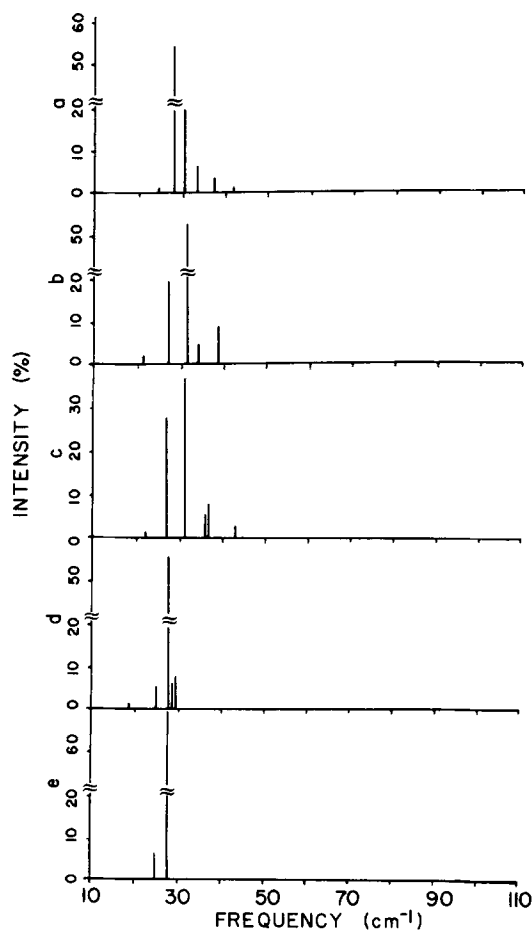

FIG. 5. LAM spectra for A–C_{74}–B. (a) A $= t_s g$, B $= gt_s$; (b) A $= D'$, B $= D$ (' indicates reverse order to the dihedral angles); (c) A $= F'_4$, B $= F_4$; (d) A $= F'_0$, B $= F_0$; (e) A $= F'_0/2$, B $= F_0/2$.

TABLE V. Calculated properties of $C_n-F_1-C_n$ and $C_{22}-F_1-C_{22}-F_1-C_{22}$ structures.[a]

Structure	v'(LAM)	β_1	I_L(A)	I_L(B)	I_L(C)	I'_T	Δv
$C_{22}-F_1-C_{22}$	95.5	0.92	9	37			
	97.2	0.94	10	22			
	101.1	0.98	18	8			
	102.4	0.99	28	. . .		82	40
$C_{35}-F_1-C_{35}$	60.6	0.92	35	10			
	61.7	0.94	15	1			
	63.3	0.96	3	29			
	64.3	0.98	1	19			
	65.4	1.00	25	15		86	27
$C_{46}-F_1-C_{46}$	46.8	0.94	2	47			
	48.0	0.97	30	4			
	50.1	1.01	31	28		89	15
$C_{22}-F_1-C_{22}-F_1-C_{22}$	95.6	0.92	2	17	20		
	96.2	0.93	3	19	36		
	98.5	0.95	29	5	. . .		
	103.8	1.00	. . .	. . .	29	80	40

[a] v'(LAM) are the LAM-1 frequencies, in cm^{-1} of those LAM-like modes with average intensity per stem $\geqslant 10\%$ of that of v(LAM)$_0$.

The designations I_L(A) and I_L(B) refer to the upper and lower stems in Fig. 6, and to the upper and middle [I_L(C) being the lower] stems in Fig. 7. (See Note added in proof.)

$I'_T = I_T$/number of stems.

Other symbols are defined in Table III.

cy to spread and the intensity to decrease, both of these depending on chain length and on the details of the terminal structures.

PLANAR ZIGZAG CHAINS CONNECTED BY FOLDS

LAM as a function of chain length and stem number

In order to obtain insights into the effects of folds on the LAM vibrations of parallel *trans* stems, we have calculated the normal modes of $C_n-F_1-C_n$ structures, where F_1 is a tight (110) fold consisting of 4 CH_2 groups.[22] The calculated results are given in Table V, which also includes the results for $C_{22}-F_1-C_{22}-F_1-C_{22}$. Atomic displacements for the most intense LAM-like modes of $C_{22}-F_1-C_{22}$ and $C_{22}-F_1-C_{22}-F_1-C_{22}$ are given in Figs. 6 and 7, respectively. The complete LAM spectra of these molecules are given in Fig. 8.

The LAM spectra show the same trend that we observed in the previous section: the envelope of LAM-like modes is broader, less intense, and more asymmetric for short stems and becomes narrower and more intense as n increases. Over the range studied, Δv and I'_T are good linear functions of n, and an extrapolation gives $\Delta v = 0$ for $n = 61$ and $I'_T = 100\%$ for $n = 85$. If we assign 2 CH_2 groups to the ends of each stem, this again suggests that the stems will behave as mass-perturbed elastic rods for a terminal mass of about 3% or less of the stem mass.

The atomic displacements in the LAM-like modes show that the stems need not all vibrate in LAM or in phase. However, the mode with the stems vibrating in phase has the lowest frequency of the most intense group, and involves fold atom displacements that are in phase with the stem ends (as if they were moving as inertial masses).[27] Although this in-phase mode may have significant intensity, it is still a small fraction of the total. It is interesting that for the three-stem system Δv is not altered even though there are more LAM-
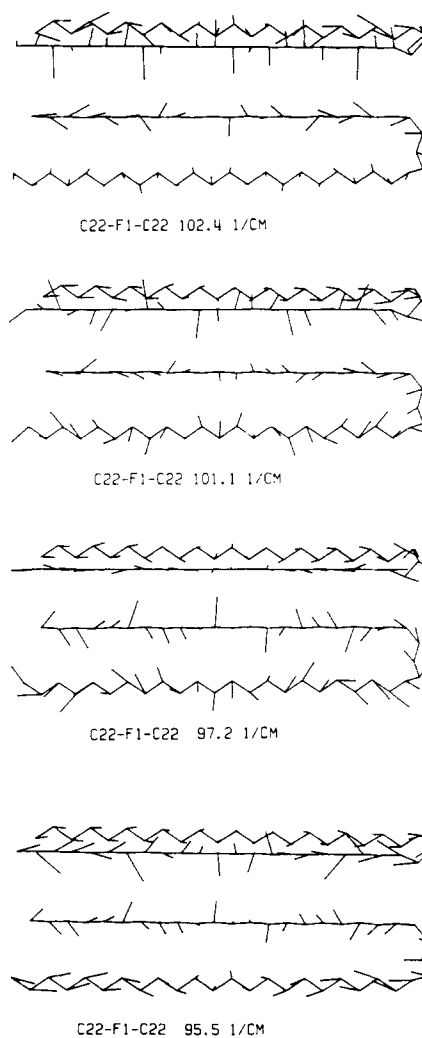
C22-F1-C22 102.4 1/CM

C22-F1-C22 101.1 1/CM

C22-F1-C22 97.2 1/CM

C22-F1-C22 95.5 1/CM

FIG. 6. Atomic displacements in most intense LAM-like modes of $C_{22}-F_1-C_{22}$.

C. Chang and S. Krimm   5532

C22-F1-C22-F1-C22   103.8 1/CM

C22-F1-C22-F1-C22   98.5 1/CM

C22-F1-C22-F1-C22   96.2 1/CM

C22-F1-C22-F1-C22   95.6 1/CM

FIG. 7. Atomic displacements in most intense LAM-like modes of C_{22}-F_1-C_{22}-F_1-C_{22}.

FIG. 8. LAM spectra of (a) C_{22}-F_1-C_{22}; (b) C_{35}-F_1-C_{35}; (c) C_{46}-F_1-C_{46}; (d) C_{22}-F_1-C_{22}-F_1-C_{22}. Intensities are average per stem.

like modes and the central stem vibrates with relatively smaller amplitudes than the outer stems, particularly with respect to out-of-plane components. It remains to be seen whether this characteristic is maintained as the number of stems increases.

LAM as a function of fold structure

Although both tight and loose folds have been proposed for lamellar crystals, the actual fold structures have yet to be determined experimentally. Expected structures have been suggested on the basis of energy calculations[20-22,24] or crystal morphology.[23] Most of these are tight folds, but loose folds have also been suggested.[21,24] We have examined the effect of fold structure on the LAM by calculating the normal modes of C_{35}-F-C_{35}, where $F = F_1, F_A, F_B$, and F'_B (F'_B is related to F_B by shortening the two arms but maintaining the turn-back geometry of the latter; cf. Tables I and VI). While F_1 is a tight fold consisting of 4 CH_2 groups, F_A, F_B, and F'_B are loose folds with 11, 23, and 15 CH_2 groups,
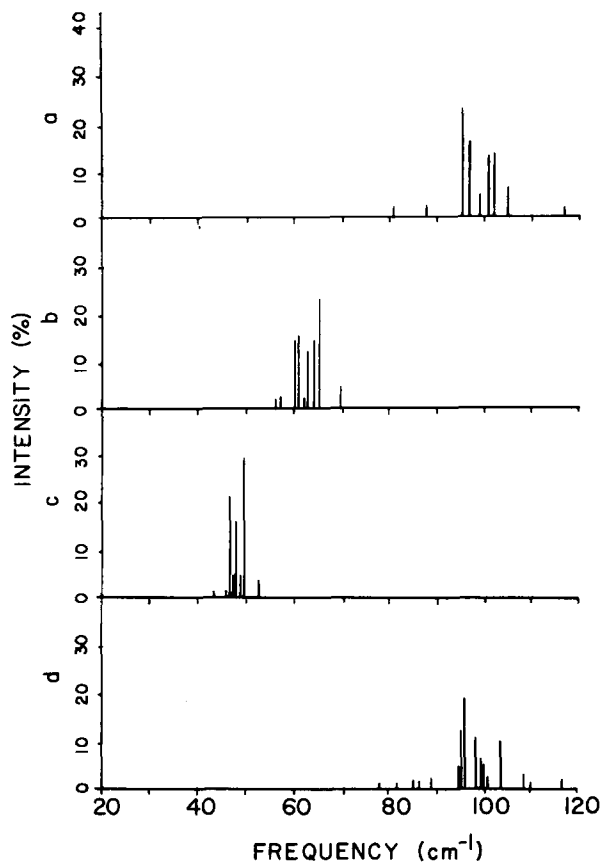
respectively. The calculated results for these structures are given in Table VI, and the LAM spectra are shown in Fig. 9.

There do not seem to be any general regularities in the LAM spectra as a function of fold length. The only obvious feature is that, whereas F_1 and F_A give rise to a closely grouped set of relatively intense LAM-like modes, F_B and

TABLE VI. Calculated properties of C_{35}-F-C_{35} structures.[a]

F	v'(LAM)	β_1	I_L(A)	I_L(B)	I'_T	Δv
F_1	60.6	0.92	35	10		
	61.7	0.94	15	1		
	63.3	0.96	3	29		
	64.2	0.98	1	19		
	65.4	1.00	25	15	86	27
F_A	60.1	0.93	69	3		
	61.7	0.94	4	19		
	62.9	0.96	2	23		
	64.8	0.99	2	20	89	20
F_B	67.5	1.03	17	19		
	70.6	1.07	21	6	83	38
F'_B	53.9	0.82	⋯	18		
	69.5	1.06	26	2		
	75.6	1.15	7	12	81	35

[a] I_L(A), I_L(B), and I'_T are the same as in Table V.

F'_B is $gtg'tgtg_2tg_3tg'tg$.
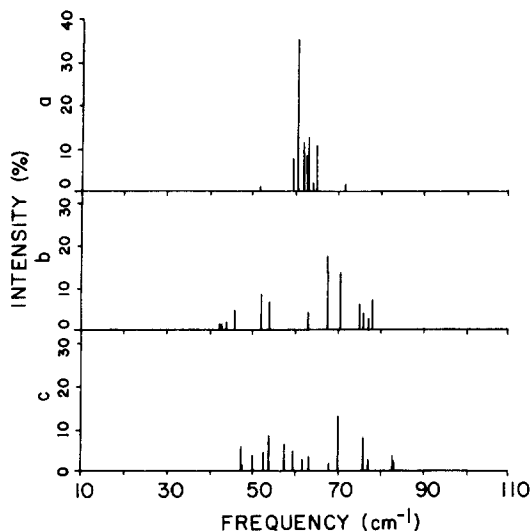
Other symbols are defined in Tables III and V.

FIG. 9. LAM spectra of $C_{35}-F-C_{35}$. (a) $F = F_A$; (b) $F = F_B$; (c) $F = F'_B$. Intensities are average per stem.

F'_B produce a widely spaced set of low intensity modes. Some of the latter are at frequencies significantly higher than $v(LAM)_0$, which seems surprising until one examines the atomic displacements[27]: in these modes fold atoms near the joint to the *trans* segments are generally moving in a direction opposite to that of the end atoms of the stem, thus in effect creating strong end forces on the stem and leading to a frequency rise [cf. Eq. (7)]. It should be noted that when the size of the fold is comparable (as in the case of the long folds) with the size of the *trans* stem, the normal modes of the whole molecule are no longer dominated by the *trans* sequence; the fold contributes its own characteristics to the normal modes. This explains why the atoms in the center region of a long fold do not "follow" the motions of those at the end of the *trans* segment, whereas the atoms in a tight fold tend to be "driven" by the motions at the end of the *trans* segment. Another way of saying this may be to note that for the F_B structure the fold, considered as a mass, comprises about 33% of the mass of a *trans* stems; if the 3% "rule" that we discussed above were to apply, we would require that $n = 383$ for the system to act like a mass-perturbed elastic rod.

The unusual appearance of two groups of LAM-like modes seen for the F_B and F'_B structures arises not only from coupling of LAM with different out-of-plane bend modes, but is probably also a consequence of the length of the fold. This characteristic undoubtedly diminishes as the *trans* stem length increases, but at present we do not know where this occurs. The dangers in such a case in attributing the LAM intensity distribution to a *trans* stem length distribution[12] are obvious.

PLANAR ZIGZAG CHAINS CONNECTED BY JOGS AND KINKS

The defects considered so far occur at the ends of *trans* stems, and would be associated with surface structures in polymer crystals. We consider now defects that could occur within a crystal, and two common ones are so-called jogs and

TABLE VII. Calculated properties of $C_{46}-J-C_{24}$ and $C_{46}-K-C_{24}$ structures.[a]

Structure	$v'(LAM)$	β_1	I_L	I'_T	Δv
$C_{46}-J-C_{24}$	C_{24}-85.7	0.91	13		
	87.7	0.93	5		
	93.4	0.99	14	40	24
	C_{46}-45.1	0.91	22		
	47.5	0.96	8		
	50.2	1.01	49	87	5
$C_{46}-K-C_{24}$	C_{24}-86.5	0.92	7		
	87.3	0.92	17	40	39
	C_{46}-48.0	0.97	38		
	52.3	1.05	16		
	52.7	1.06	19	85	16

[a] I_L and I_T are related to quantities for unperturbed C_{24} and C_{46}. Other symbols are defined in Tables III and V.

kinks. A jog consists of a transverse dislocation of the chain axis, usually accompanied by a rotation of the plane of the zigzag. A kink involves no change in these quantities. The jog and kink conformations that we used are given in Table I, and the calculated results are presented in Table VII and Fig. 10 for $C_{46}-J-C_{24}$ and $C_{46}-K-C_{24}$ structures.

Our calculations confirm the results of previous studies,[15] viz., that a local internal defect completely disrupts the LAM vibration of the full molecule. The molecule now vibrates with two sets of LAM modes, each localized in one of the *trans* stems.[27]

In addition, we find that the effect of the asymmetry of the defect on the LAM modes of the two stems is significant.[27] In the case of $C_{46}-K-C_{24}$ the LAM vibration in the C_{24} segment penetrates well into the kink, while the LAM in C_{46} terminates at the end of the C_{46} segment. This is probably because the structure of the kink changes the direction of the C_{24} segment smoothly but that of the C_{46} segment abruptly. This undoubtedly accounts for β_1 values greater than 1 for the C_{46} segment. In the case of $C_{46}-J-C_{24}$ the
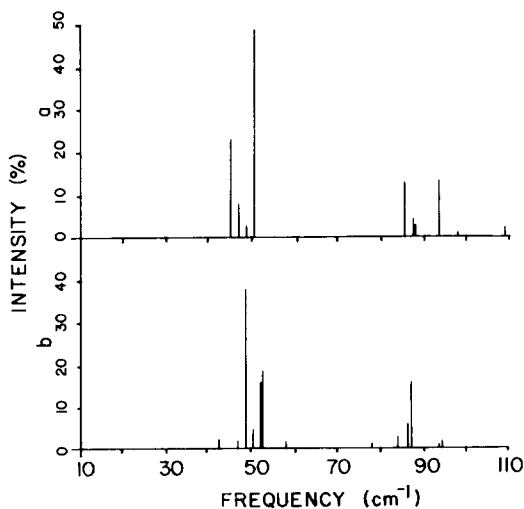

FIG. 10. LAM spectra for (a) $C_{46}-J-C_{24}$ and (b) $C_{46}-K-C_{24}$.

directional changes are not as abrupt, and the specific effects on the LAM modes due to the defect are more obvious. In particular, since the LAM vibration involves in-plane bond stretching and angle bending, which are at higher frequencies than the out-of-plane primarily torsional motions, whenever the mode is primarily a LAM of the C_{46} segment the C_{24} segment vibrates only with out-of-plane motions, whereas modes that are primarily a LAM of the C_{24} segment usually exhibit small longitudinal displacements in the C_{46} segment. Thus, although each group of LAM modes is effectively confined to one of the *trans* segments, this does not mean that either segment vibrates as an independent chain.

FORCE PERTURBATIONS

At the beginning of the paper we raised the question of whether the perturbed elastic rod model provided reliable answers for the effects of force and mass perturbations on the LAM mode. We now try to answer these questions on the basis of normal mode calculations.

We first calculated the effect of end forces on C_{22}, and the frequencies and relative intensities of ν(LAM) as a function of force constant are given in Fig. 11. As for the unperturbed molecule, there is only a single LAM mode; no frequency spreading occurs as a result of the force perturbation. The frequency increases with f, and follows the approximate relation, Eq. (7), until $f \cong 0.1$ mdyn/Å, i.e., $2fL/\pi^2AE \leqslant 0.1$. Beyond this value it falls below that predicted from Eq. (7), as expected from the complete treatment.[5] The intensity variation also follows Eq. (14) until $f \cong 0.1$ mdyn/Å, after which the intensity falls faster than predicted by Eq. (14). It is not clear whether this is a general trend, because a normal mode calculation of C_{58} gave a different result: for $f = 0.0488$ mdyn/Å ($2fL/\pi^2AE = 0.135$) we found that $\nu = 47.1$ cm^{-1}, compared to 44.7 cm^{-1} predicted by Eq. (7), but the intensity ratio was 0.92, compared to 0.87 predicted by Eq. (14). If indeed for longer chains the intensity does not drop as rapidly as predicted by Eq. (14), this could account for the more nearly constant LAM intensity as a function of chain length found for n-paraffins.[13]
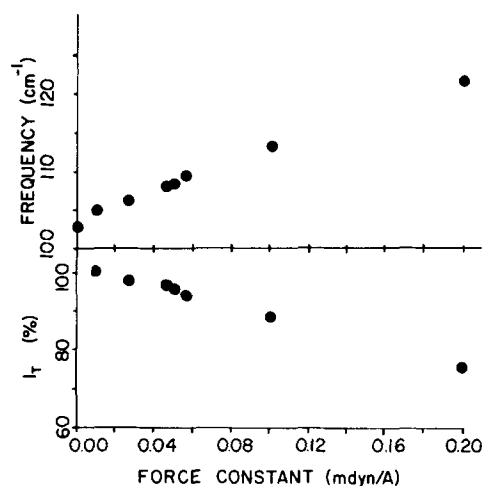

FIG. 11. Frequency and relative intensity of LAM of C_{22} as a function of end force constants.

We turn next to the effects of forces on defect structures. As an initial study we calculated the normal modes of $F_C^*-C_n-F_C^\dagger$ when forces represented by $f = 0.0488$ mdyn/Å act on the end structures. The results are given in Table VIII and the spectra are shown in Fig. 12. Atomic displacements for $F_C^*-C_{22}-F_C^\dagger$ are given in Fig. 13. In the presence of interactions the frequencies of some LAM-like modes shift to higher values whereas others remain nearly the same. Intensity distributions also change. Thus, for $F_C^*-C_{22}-F_C^\dagger$ the frequency of the most LAM-like mode at 82.3 cm^{-1} (Table III and Fig. 2) shifts to 84.0 cm^{-1} when parallel forces act on atoms 4 and 31, and to 83.4 cm^{-1} when forces act on atoms 4 and 32, but the frequency of the 89.1 cm^{-1} mode (Fig. 2) hardly changes. The intensity change, from 23% to 30%–31%, can be understood by comparing the atomic displacements in Figs. 2 and 13: as a result of the end forces the atoms have a larger longitudinal component to their displacements. In general, the extent of response to the forces depends on how large a longitudinal component existed at the atoms to which the forces are applied. In the above example

TABLE VIII. Calculated properties of $F_C^*-C_n-F_C^\dagger$ with end forces.[a]

Structure	Forces	ν(LAM)	β_1	I_L	I_T'	$\Delta\nu$
$F_C^*-C_{22}-F_C^\dagger$	4, 31; $\parallel$[b]	84.0	0.81	31		
		89.1	0.86	18	65	65
$F_C^*-C_{22}-F_C^\dagger$	4, 32; $\parallel$	83.4	0.81	30		
		89.2	0.86	21	68	65
$F_C^*-C_{58}-F_C^\dagger$	4, 68; $\parallel$	37.6	0.95	28		
		38.1	0.97	37	84	19
$F_C^*-C_{74}-F_C^\dagger$	4, 84; $\parallel$	28.8	0.93	21		
		30.2	0.98	31		
		32.4	1.05	25	83	11
$F_C^*-C_{74}-F_C^\dagger$	4, 84; $\perp$	27.8	0.89	29		
		28.6	0.93	36	85	17

[a] Symbols are defined in Tables III and V.

[b] Forces on atoms 4 and 31 (counting from the right end of the molecule in Fig. 2), and parallel to the all-*trans* axis.
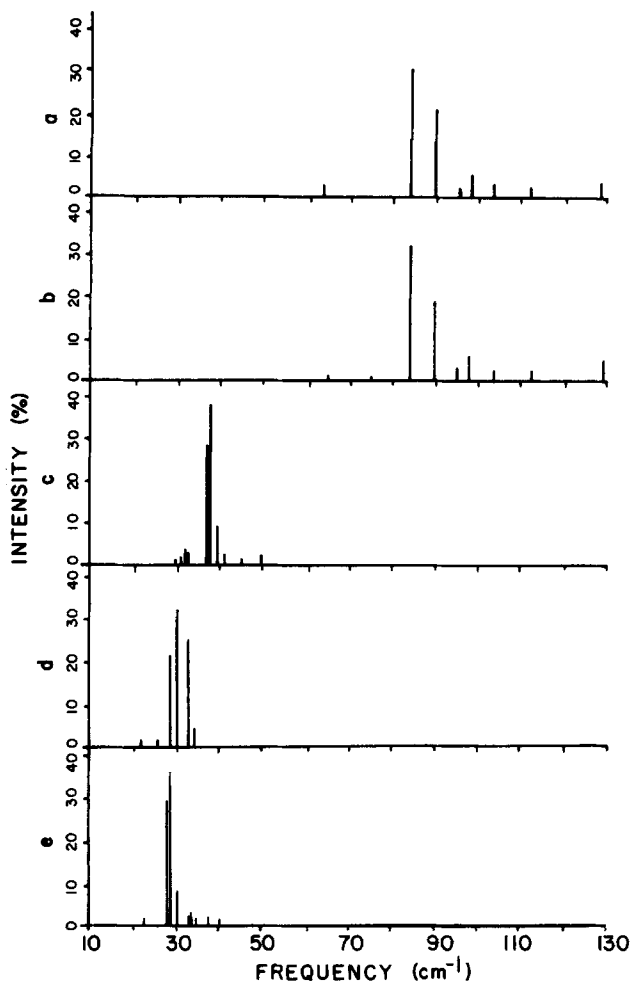
FIG. 12. LAM spectra of $F_C^*-C_n-F_C^\dagger$ with forces on terminal structures. (a) $n = 22$, parallel forces on atoms 4 and 31; (b) $n = 22$, parallel forces on atoms 4 and 32; (c) $n = 58$, parallel forces on atoms 4 and 68; (d) $n = 74$, parallel forces on atoms 4 and 84; (e) $n = 74$, perpendicular forces on atoms 4 and 84.
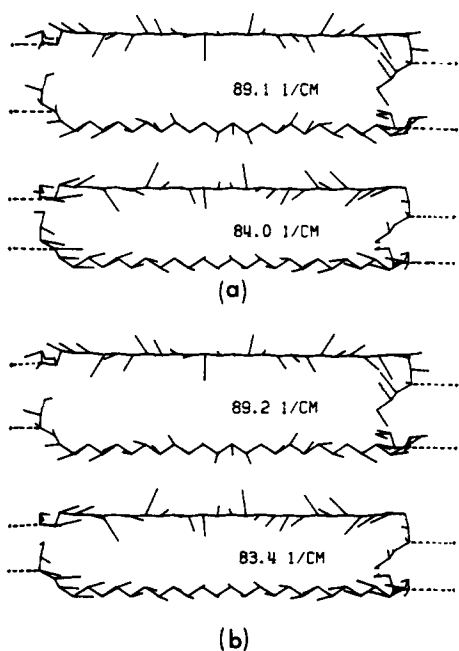

FIG. 13. Atomic displacements in most intense LAM-like modes of $F_C^*-C_{22}-F_C^\dagger$ with end forces on (a) atoms 4 and 31, and (b) atoms 4 and 32.

(cf. Fig. 2), there is a much larger longitudinal motion of atom 31 than atom 32 in the 82.3 cm^{-1} mode, and therefore the frequency is shifted more in the former case than the latter. For the 89.1 cm^{-1} mode the displacements of atoms 31 and 32 are about equal and small; so this mode is hardly affected.

The situation for $F_C^*-C_{58}-F_C^\dagger$ is more complex. The most LAM-like mode at 36.2 cm^{-1} ($I_L = 46$) shifts to 38.1 cm^{-1} ($I_L = 37$) and changes character significantly,[27] while the 37.7 cm^{-1} mode retains most of its character, undergoing almost no frequency change (36.6 cm^{-1}), but its intensity changes from 12% to 28%. For $F_C^*-C_{74}-F_C^\dagger$, the original strong mode at 29.0 cm^{-1} ($I_L = 64$) and much weaker mode at 27.7 cm^{-1} ($I_L = 5$) are replaced by three less intense modes at 28.8 ($I_L = 21$), 30.2 ($I_L = 31$), and 32.4 cm^{-1} ($I_L = 25$). In these three $F_C^*-C_n-F_C^\dagger$ cases one effect of the longitudinal forces has been to increase the total intensity in the group of relatively strong LAM-like modes. This is again a result of an increase in the longitudinal displacement components under the action of the forces, a mechanism, incidentally, that is not available to an elastic rod.

An interesting question concerns the effects of forces applied at the ends but perpendicular to the axis of the *trans* stem. As might be expected, there is no effect on *trans* C_{22}. But, as shown in Table VIII and Fig. 12 for $F_C^*-C_{74}-F_C^\dagger$, this is no longer true for a molecule with defects. The original spectrum of $F_C^*-C_{74}-F_C^\dagger$, (Fig. 3) is perturbed by the lateral interactions (Fig. 12), and in a way different from that due to the longitudinal interactions. It is interesting that, whereas longitudinal interactions lead to an upshift in the intensity-weighted mean of the group of relatively strong LAM-like modes, from 28.9 to 30.7 cm^{-1} for $F_C^*-C_{74}-F_C^\dagger$, lateral interactions in this case lead to a small downshift, from 28.9 to 28.5 cm^{-1}. If this is generally true, then it has important implications with respect to the effects on the LAM of the stems of lateral interactions between folds at the surfaces of polyethylene single crystals.

We have also calculated the effects of a longitudinal force acting on either of two central atoms in the fold of a $C_{22}-F_C-C_{22}$ structure.[27] The frequency pattern (with $\Delta v = 60$ cm^{-1}; cf. 40 cm^{-1} for $C_{22}-F_1-C_{22}$, Table V) is not as significantly altered by the end force as was the case for the $F_C^*-C_n-F_C^\dagger$ structures, but similar frequency shifts occur as a function of the longitudinal displacement of the atom to which the force is applied.

In all of the above calculations the pseudo bond was attached to a mass of 10^4 amu. When this mass was reduced to 138 amu (that of a decalin molecule), the effect on the LAM-like modes of $F_C^*-C_{74}-F_C^\dagger$ was to produce only a minor redistribution of intensities. Thus, an adsorbed molecule on the surface of a polymer crystal should manifest itself primarily through its interaction forces with surface structures.

To summarize, normal mode calculations show that force perturbations can have complex effects that depend on the unperturbed motion of the atom on which the force acts. In general, the frequencies of LAM-like modes are raised by the action of longitudinal end forces: for C_n chains this in-

crease follows Eq. (7) for small f and departs from this relation as predicted[5] for large f; for chains with end structures the frequency increase probably does not follow these relations until the stem is long enough for the terminal structure to behave like a point mass. Even in the latter case the details are likely to be determined by the specific atom motions in the end structure as well as by the distribution of forces; a simple dependence on L [Eq. (7) and Ref. 5] may not be valid. The intensities of LAM-like modes seem to behave in an even more complex fashion under the influence of force perturbations. For C_N chains the intensity decreases with f and L, but apparently not as rapidly as predicted by Eq. (14). For chains with terminal structures the total intensity of the group of relatively strong LAM-like modes is increased by the application of longitudinal forces. The observed frequency and intensity of a LAM band for a *trans* chain with end defects is thus seen to represent a balance between a number of factors.

MASS PERTURBATIONS

The elastic rod model predicts that a small point mass added to the end of the rod will cause the frequency to decrease [Eq. (7)] and the intensity to increase [Eq. (14)]. We have examined this prediction by normal mode calculations on C_{22} with masses of 5–65 amu added to one or both ends, and the results are shown in Fig. 14. The frequencies are found to decrease linearly up to ~ 35 amu, following Eq. (7) for small masses; beyond ~ 35 amu Eq. (7) would overestimate the mass effect. The intensities are also found to decrease with mass, opposite to the prediction of Eq. (14). The calculations indicate, however, that this is accompanied by an increase in intensity of some non-LAM modes near the LAM frequencies. Although it is claimed[16] that the sum of these intensities is conserved, it seems that the isotope intensity sum rule[28] ($\Sigma I_i/v_i^2 = \Sigma I_j'/v_j'^2$, where the prime indicates the isotopic species) would require that, since frequencies are lowered by increasing masses, the intensity sum should also decrease.

The effects of mass perturbations were next tested on $F_1-C_{22}-F_1$ and $F_C^*-C_{74}-F_C^+$ structures. The results are
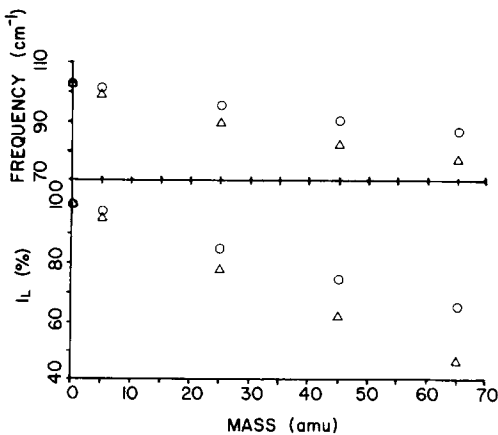
TABLE IX. Calculated properties of $F-C_n-F$ structures with added masses.[a]

Structure	v'(LAM)	β_1	I_L	I_T	Δv
$F_1-C_{22}-F_1$	80.1	0.78	13		
	94.4	0.92	45		
	96.2	0.93	12	82	38
$M_1F_1-C_{22}-F_1M_1$[b]	94.3	0.92	48	77	38
$M_CF_C^*-C_{74}-F_C^+M_C$[c]	28.8	0.93	47		
	30.7	0.99	18	85	13
$BrF_C^*-C_{74}-F_C^+Br$[d]	27.3	0.94	10		
	28.6	0.99	47	79	20
$BrF_C^*-C_{74}-F_C^+Br$[e]	23.3	0.80	9		
	25.3	0.87	24		
	25.5	0.88	13		
	27.8	0.96	10	68	15
$BrF_C^*-C_{74}-F_C^+Br$[f]	23.6	0.81	13		
	24.7	0.85	14		
	25.4	0.88	16		
	26.0	0.90	18	67	14

[a] Symbols are defined in Tables III and V.
[b] $M_1 = 310$ amu, and is added to the end atoms.
[c] $M_C = 1036$ amu, and is added to the end atoms.
[d] $Br = 80$ amu, and is located on atoms 3 and 84.
[e] Br is located on atoms 5 and 82.
[f] Br is located on atoms 6 and 81.

shown in Table IX, the spectra are given in Figs. 15 and 16, respectively, and the atomic displacements for the $F_1-C_{22}-F_1$ structure are illustrated in Fig. 17. We, of course, recognize that these calculations only approximate the case, such as addition of Br to folds of polyethylene single crystals, in which the additional mass resides in a separate atom, but since the C–Br stretching frequency is so much higher than the LAM frequency, we believe that the former will be minimally excited at the latter and the pure mass effect will predominate.

In general, the frequency decrease due to the added mass is not as large as is predicted by the elastic rod model.
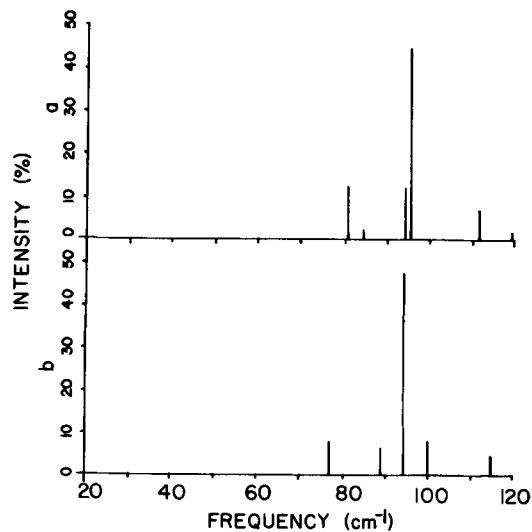

FIG. 14. Frequency and relative intensity of LAM of C_{22} as a function of point masses at (O) one end and (△) both ends of the chain.

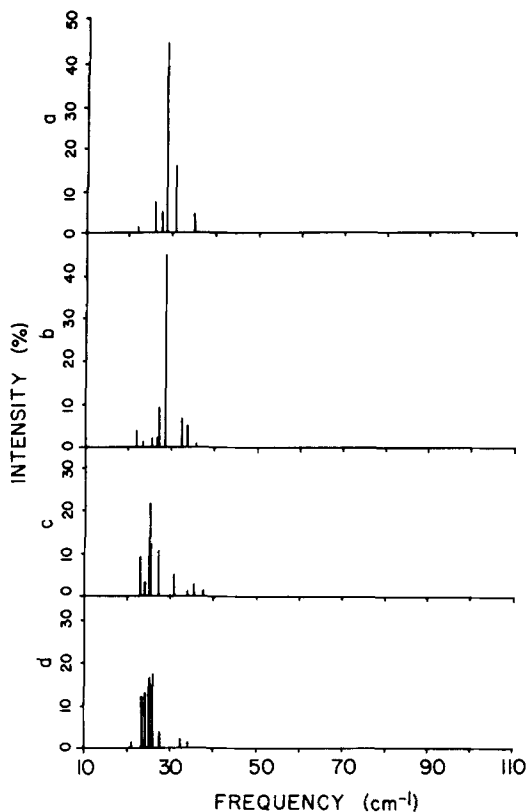FIG. 15. LAM spectra of (a) $F_1-C_{22}-F_1$ and (b) $M_1F_1-C_{22}-F_1M_1$, $M_1 = 310$ amu.[a]

FIG. 16. LAM spectra of (a) $M_C F_C^*-C_{74}-F_C^\dagger$, $M_C M_C = 1036$ amu; (b) $BrF_C^*-C_{74}-F_C^\dagger$ Br, Br on atoms 3 and 84; (c) $BrF_C^*-C_{74}-F_C^\dagger$ Br, Br on atoms 5 and 82; (d) $BrF_C^*-C_{74}-F_C^\dagger$ Br, Br on atoms 6 and 81.

FIG. 17. Atomic displacements in most intense LAM-like modes of $F_1-C_{22}-F_1$ and $M_1F_1-C_{22}-F_1M_1$, $M_1 = 310$ amu.

Thus, for $F_1-C_{22}-F_1$ the frequency drops by only 1.9 cm^{-1} for end masses of 310 amu, although the elastic rod model predicts[6] a decrease of a few tens of cm^{-1}. It seems that the crucial factor is how close the increased mass is to the end of the *trans* stem. For example, as Fig. 17 indicates, putting masses of 310 amu at the ends of a $F_1-C_{22}-F_1$ structure inhibits the motion of the end atom in the 96.2 cm^{-1} mode (which was large in the unperturbed system), but it does not change substantially the motions of the end atoms of the C_{22} stem. This is seen even more clearly on examining the atomic displacements in the $F_C^*-C_{74}-F_C^\dagger$ structure[27]: when Br
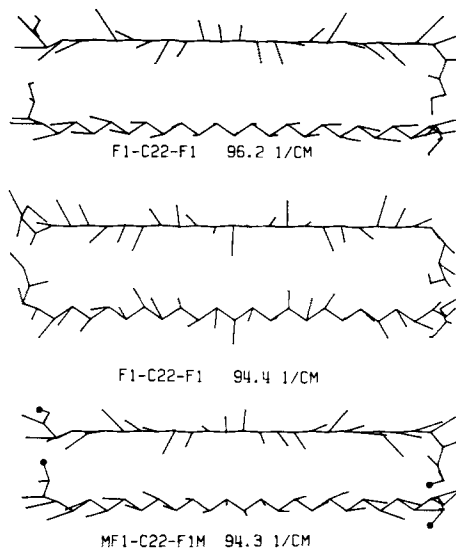
masses are added to atoms 3 and 84 the vibrations of the *trans* stem are hardly affected (and the spectra are hardly changed; cf. Figs. 3 and 16), but when the masses are added to atoms 5 and 82 or 6 and 84 the vibrations of the *trans* stems (and the spectra; cf. Fig. 16) are significantly modified. It is as if a mass placed on an atom near the end of the *trans* stem has a strong effect on "clamping" the LAM-like vibration that, as we have seen, penetrates beyond the end of the stem and into the terminal structure. We note that the LAM spectra of $F_C^*-C_{74}-F_C^\dagger$ with Br atoms near the ends of the stem have β_1 values near 0.9, which is the value predicted by the elastic rod model for Br masses added to the ends of a C_{74} chain.[6]

We have made similar calculations for structures with folds, viz., $C_{22}-F_1-C_{22}$ and $C_{22}-F_1-C_{22}-F_1-C_{22}$,[27] of which the results for the latter are given in Table X, the spectra in Fig. 18, and atomic displacements for one case in Fig. 19. Effects similar to those discussed above can be seen in this system. A comparison of Figs. 7 and 19 shows that addition of masses to atoms 25 and 50 has produced little change in

TABLE X. Calculated properties of $C_{22}-F_1-C_{22}-F_1-C_{22}$ structures with added Br masses.[a]

Masses	v'(LAM)	β_1	I_L(A)	I_L(B)	I_L(C)	I'_T	Δv
25, 50[b]	94.8	0.92	20	9	...		
	97.0	0.94	25	3	8		
	98.6	0.96	9	...	19		
	103.5	1.01	...	...	33	76	43
24, 50	93.4	0.91	21	...	2		
	93.8	0.91	5	22	2		
	98.5	0.96	26	...	...		
	103.4	1.01	...	...	36	73	48
25, 51	95.1	0.92	15	32	...		
	98.1	0.95	32	11	...		
	102.2	0.99	...	...	78	80	23

[a] Symbols are defined in Tables III and V.
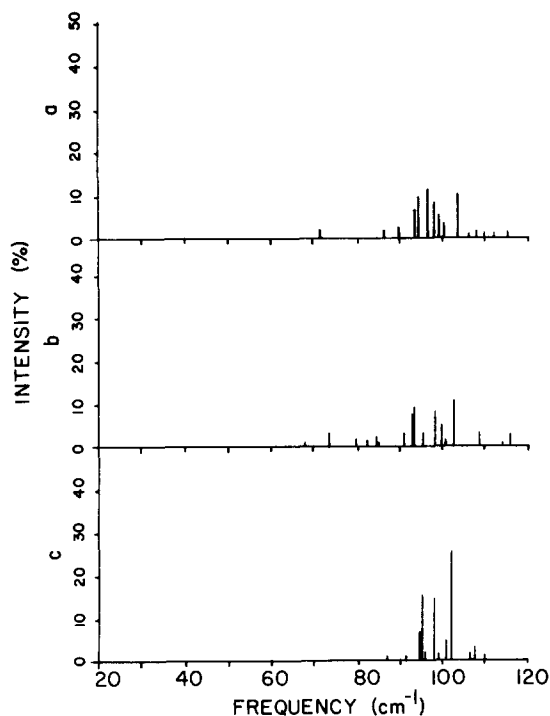[b] Atoms whose masses have been increased by 80 amu.

FIG. 18. LAM spectra for C_{22}-F_1-C_{22}-F_1-C_{22} with Br masses on (a) atoms 25 and 50; (b) atoms 24 and 50; (c) atoms 25 and 51.

FIG. 19. Atomic displacements in the most intense LAM-like modes of C_{22}-F_1Br-C_{22}-F_1Br-C_{22} with Br masses on atoms 25 and 50.

the displacements in the 103.8 cm^{-1} mode but has had larger effects on the other three modes (cf. also Tables V and X). The overall spectra (Figs. 8 and 18) are not too dissimilar. Addition of mass to atom 24, closer to the end of the *trans* stem, produces larger effects.

Mass perturbations, therefore, can have the effect of reducing the LAM frequency as well as intensity, the latter being contrary to the predictions of the elastic rod model [Eq. (14)]. Bands in general will be broadened, as happens whenever defects are introduced into the system. Effects are enhanced when masses are added within 2 CH$_2$ units of the ends of the *trans* stem.

CONCLUSIONS

Our normal mode analyses of planar zigzag stems of varying length terminated or connected by various fold structures show that the perturbed elastic rod model has a limited validity. This arises from the fact that in the elastic rod model the LAM occurs as a single mode comprised entirely of longitudinal displacements, whereas in the real molecule the coupling with the nonregular structures causes the LAM-like displacements to be distributed among modes covering a range of frequencies and having transverse displacements as well. Only when the terminal structures comprise less than ~3% of the mass of the stem can they be considered as point masses and the stem frequency treated in terms of the perturbed rod theory.[6] In any case, the presence of point masses leads to decreases in the LAM intensity whereas the elastic rod predicts the opposite.

The force field we have used reproduces very well the observed LAM frequencies and intensities of C_n planar zigzag chains for $n \geqslant 36$. These calculations serve to define the
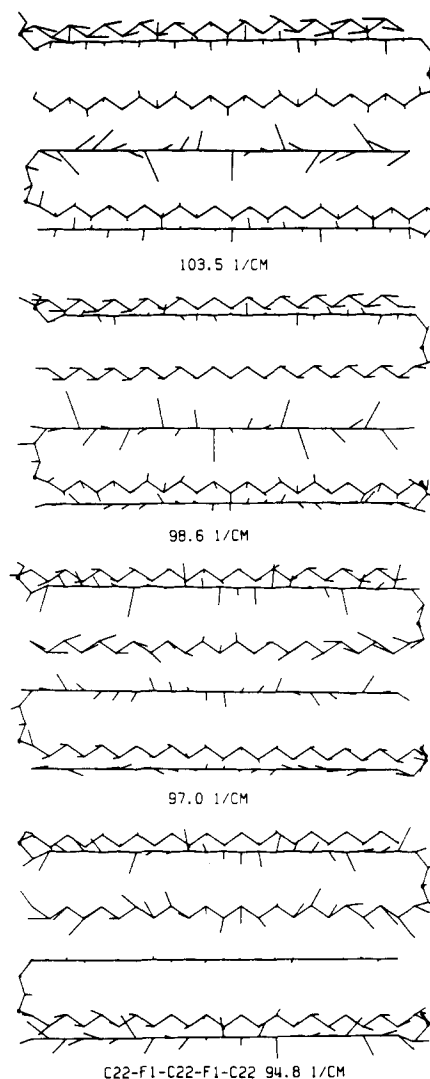
parameters of unperturbed chains. When fold structures are added to such stems, the LAM frequency of the perturbed stem can be higher or lower than the unperturbed, depending on the conformation of the fold. The coupling of the stem vibration to the fold is not interrupted by an intervening gauche bond, except that bonds beyond the first three after the joint have relatively little effect on the LAM. In any case, the frequency range over which LAM-like modes are found increases significantly, and the total intensity of the major bands decreases, as compared to the unperturbed LAM. Only when these structures contain ~3% or less of the total mass of the stem does the frequency range collapse to a single line (determined by the mass perturbation) and the intensity become equivalent to that for the unperturbed stem. Jogs and kinks within a planar zigzag chain lead to essential decoupling of LAM modes in the two segments, although these still cannot be considered to vibrate independently.

When the above kinds of structures are subject to perturbations such as end forces or masses the LAM frequency is raised or lowered, respectively. The specific change is sensitive to the original motion of the atom on which the force

acts or to which the mass is attached, being of course minimal if that motion in the normal mode is small. In either case the LAM intensity always drops in the presence of the perturbations.

In general, the LAM-1 frequency alone is not sufficient to provide information on the end structures and the perturbations, since cancellation of different effects can occur. The half width of the LAM band does not necessarily represent the distribution of stem lengths; it is also determined by the end structures and the length of the stem. The intensity of the LAM is the parameter that is most sensitive to the perturbations. Therefore, only an analysis of all three of these quantities can reliably determine the thickness of the crystalline core.

Note added in proof. The intensities associated with planar zigzag chain connected by folds, such as are given in Tables V and VI, were calculated on the assumption that the vibrations in each stem are independent. While such decoupling may be appropriate in a folded chain polymer crystal, it is not strictly true for our model system. For these cases, $I_L = [\Sigma_X I_L^{1/2}(X)]^2$, where the signs of $I_L^{1/2}(X)$ are given by the relative phases of the vibrations in the stems. Thus for C_{22}–F_1–C_{22}, as can be seen from Fig. 6, the relative signs are 95.5: $+$, 97.2: $-$, 101,1: $-$. Similarly, the signs for the other structures are (in the order of increasing frequencies) C_{35}–F_1–C_{35}: $+$, $-$, $-$, $+$, $-$; C_{46}–F_1–C_{46}: $+$, $+$, $-$; C_{22}–F_1–C_{22}–F_1–C_{22}: $+$ $+$, $+$ $-$, $-$; C_{35}–F_A–C_{35}: $+$, $+$, $-$, $-$; C_{35}–F_B–C_{35}: $+$, $-$; C_{35}–F'_B–C_{35}: $-$, $+$. The I_L distributions vary somewhat from those given in Figs. 8 and 9, with relatively higher intensity concentrated in the lowest (in-phase) frequency, but the general conclusion given in the text are essentially unchanged.

ACKNOWLEDGMENTS

[1] S. Mizushima and T. Shimanouchi, J. Am. Chem. Soc. **71**, 1320 (1949).
[2] R. F. Schaufele and T. Shimanouchi, J. Chem. Phys. **47**, 3605 (1967).
[3] H. G. Olf, A. Peterlin, and W. L. Peticolas, J. Polym. Sci. Polym. Phys. Ed. **12**, 359 (1974).
[4] G. R. Strobl and R. Eckel, J. Polym. Sci. Polym. Phys. Ed. **14**, 913 (1976).
[5] S. L. Hsu and S. Krimm, J. Appl. Phys. **47**, 4265 (1976).
[6] S. L. Hsu, G. W. Ford, and S. Krimm, J. Polym. Sci. Polym. Phys. Ed. **15**, 1769 (1977).
[7] S. L. Hsu and S. Krimm, J. Appl. Phys. **48**, 4013 (1977).
[8] S. Krimm and S. L. Hsu, J. Polym. Sci. Polym. Phys. Ed. **16**, 2105 (1978).
[9] C. Chang and S. Krimm, J. Polym. Sci. Polym. Phys. Ed. **17**, 2163 (1979).
[10] A. Peterlin, J. Appl. Phys. **50**, 838 (1979).
[11] A. Peterlin, J. Polym. Sci. Polym. Phys. Ed. **20**, 2329 (1982).
[12] R. G. Snyder, S. J. Krause, and J. R. Scherer, J. Polym. Sci. Polym. Phys. Ed. **16**, 1593 (1978).
[13] G. R. Strobl and R. Eckel, Coll. Polym. Sci. **258**, 570 (1980).
[14] T. Shimanouchi and M. Tasumi, Ind. J. Pure Appl. Phys. **9**, 958 (1971).
[15] D. H. Reneker and B. Fanconi, J. Appl. Phys. **46**, 4144 (1975).
[16] J. Mazur and B. Fanconi, J. Chem. Phys. **71**, 5069 (1979).
[17] B. Fanconi and J. Crissman, J. Polym. Sci. Polym. Lett. Ed. **13**, 421 (1975).
[18] S. Krimm, Ind. J. Pure Appl. Phys. **16**, 335 (1978).
[19] G. R. Strobl, J. Polym. Sci. Polym. Phys. Ed. **21**, (1983) (in press).
[20] P. Corradini, V. Petraccone, and G. Allegra, Macromolecules **4**, 770 (1971).
[21] T. Oyama, K. Shiokawa, and Y. Kawamura, Polymer J. **9**, 1 (1977).
[22] P. E. McMahon, R. L. McCullough, and A. A. Schlegel, J. Appl. Phys. **38**, 4123 (1967).
[23] D. C. Bassett, *Principles of Polymer Morphology* (Cambridge University, Cambridge, 1981).
[24] T. Oyama, K. Shiokawa, and T. Ishimaru, J. Macromol. Sci. Phys. B **8**, 229 (1973).
[25] R. G. Snyder, J. Chem. Phys. **47**, 1316 (1967).
[26] L. A. Woodward and D. A. Long, Trans. Faraday Soc. **45**, 1131 (1949).
[27] C. Chang, Ph.D. Thesis, University of Michigan, 1983.
[28] E. B. Wilson, Jr., J. C. Decius, and P. C. Cross, *Molecular Vibrations* (McGraw-Hill, New York, 1955), p. 192.

5540   J. Appl. Phys., Vol. 54, No. 10, October 1983

C. Chang and S. Krimm   5540